Separation Science and Technology
Publication details, including instructions for authors and subscription information:
http://www.informaworld.com/smpp/title~content=t713708471

Diffusive Salt Permeation Properties of Charged Membranes at Low Charge Densities. Experimental Verification of a Space Charge Model

L. Martinez[a]; A. Hernandez[a]; F. Tejerina[a]
[a] DEPARTAMENTO DE FISICA APLICADA II (TERMOLOGIA), FACULTAD DE CIENCIAS UNIVERSIDAD DE VALLADOLID, VALLADOLID, SPAIN

To cite this Article Martinez, L. , Hernandez, A. and Tejerina, F.(1988) 'Diffusive Salt Permeation Properties of Charged Membranes at Low Charge Densities. Experimental Verification of a Space Charge Model', Separation Science and Technology, 23: 1, 243 — 259
To link to this Article: DOI: 10.1080/01496398808057646
URL: http://dx.doi.org/10.1080/01496398808057646

SEPARATION SCIENCE AND TECHNOLOGY, **23**(1-3), pp. 243-259, 1988

Diffusive Salt Permeation Properties of Charged Membranes at Low Charge Densities. Experimental Verification of a Space Charge Model

L. MARTINEZ, A. HERNANDEZ, and F. TEJERINA

DEPARTAMENTO DE FISICA APLICADA II (TERMOLOGIA)
FACULTAD DE CIENCIAS
UNIVERSIDAD DE VALLADOLID
47071 VALLADOLID, SPAIN

Abstract

We characterize and interpret the response of some microporous membranes separating two electrolytic aqueous solutions. This is done by following a transport model whose validity is tested by comparing experimental and predicted values of saline permeability. The basic equations of the transport model (the coupled Nernst-Planck and Poisson-Boltzmann equations) are numerically solved. The concentration and potential membrane profiles are also obtained for different pore radius and solution concentrations.

INTRODUCTION

Electrolyte transport through charged membranes has been extensively studied. Most of this work has been carried out with membranes of high charge densities. Such membranes represent highly nonideal systems, which complicates the interpretation of the experimental results. Also, in electroneutral transport, these membranes become virtually impermeable to low concentrated electrolyte solutions because the coions are almost absolutely excluded from the membrane phase. This limits the useful experimental range to comparatively high concentrations of the electrolyte.

Some of these difficulties can be avoided when the charge density is low. Then the measurements can include operations with dilute solutions, whose treatment is easier.

In the present work, two polycarbonate microporous membranes (pore diameters: 0.1 and 0.003 μm) are studied when they separate two electrolytic aqueous solutions (of LiCl or $MgCl_2$) whose concentrations go from 0.1 to 100 mol/m^3. Their properties involving the diffusional transport of electrolytes are also analyzed. This is done within the framework of a transport model that assumes the membrane is an array of cylindrically-equal capillary pores with a uniform surface charge density. This study leads to the numerical resolution of the Nernst-Planck and Poisson-Boltzmann equations.

The exact solution of the Nernst-Planck and Poisson-Boltzmann equations for membrane systems containing two ions has received much attention (*1*, *2*). Attempts to solve these equations analytically resulted in asymptotic solutions for special cases. Numerical procedures, such as those employed here, provide accurate, exact solutions for virtually all realistic input parameters, and provide a versatility and ease of use not obtainable with analytical approaches. Ever since Cohen and Cooley (*3*) first applied such procedures (often referred to as digital simulations) to membrane problems, they have found widespread use in a number of areas (*2*).

The simulation procedure we developed has allowed us to 1) test the validity of the space-charge model for electrolyte transport through charged membranes with capillary pores by comparing the experimental values of saline permeability with those calculated by means of the model; and 2) to determine the axial and radial profiles of concentration and electric potential of a membrane pore in steady-state conditions. These examples illustrate some of the capabilities of the technique.

THEORY

A number of physical situations arise in which a charged porous membrane separates two solutions of the same electrolyte but at different concentrations. The effects of double layers on steady-state transport through charged pores can be studied by means of the Poisson-Boltzmann equation for electrostatic potential in the layers, together with the Nernst-Planck equation for ionic fluxes (*4*).

In this way, when the pore length, l, is much bigger than its radius, $\bar{a}$, the flux of i species, J_i, through the pore is described by

$$J_i(r,x) = -D_i\left[\frac{\partial c_i(r,x)}{\partial x} + \frac{z_i F}{RT}\, c_i(r,x)\, \frac{\partial \phi(r,x)}{\partial x}\right] \qquad (1)$$

where r and x are the radial and axial coordinates, $c_i(r,x)$ is the concentration of the i ion, D_i is its diffusion coefficient, z_i is its charge number, T is the temperature, R is the gas constant, and F is the Faraday constant.

The total electrical potential, $\phi(r,x)$, can be written as

$$\phi(r,x) = \frac{RT}{z_+F}\psi(r,x) + E_m(x) \tag{2}$$

where $\psi(r,x)$ is the electrostatic potential arising from the double layer in dimensionless form, while $E_m(x)$ is the potential whose difference between the bulk solutions on each side of the membrane (the membrane potential) can be measured.

The concentration, $c_i(r,x)$, of the i ion follows a Boltzmann distribution,

$$c_i(r,x) = \nu_i\bar{c}(x)\exp\left(-\frac{z_i}{z_+}\psi(r,x)\right) \tag{3}$$

where ν_i is the stoichiometric coefficient of the i ion and $\bar{c}(x)$ can be interpreted (5) as the equivalent bulk concentration that would be at equilibrium with the solution in the pore cross section at axial position x. The ends of the pores are assumed to be at equilibrium with the adjacent bulk solutions.

The calculation of salt and charge fluxes by Eq. (1) requires (6) solution of the Poisson-Boltzmann equation,

$$\frac{1}{\xi}\frac{\partial}{\partial\xi}\left(\xi\frac{\partial}{\partial\xi}\right) = \left(\frac{\bar{a}}{\lambda}\right)^2\frac{z_+}{z_+ - z_-}\left[e^{-z_-\psi/z_+} - e^{-\psi}\right] \tag{4}$$

where $\xi = r/\bar{a}$ and $\lambda(x)$ is the equivalent Debye length defined by

$$\lambda^2(x) = \frac{\varepsilon RT}{F^2\sum_i z_i\nu_i\bar{c}(x)} \tag{5}$$

ε being the dielectric constant.

Equation (4) must be solved with the boundary conditions given by:

a) The surface charge density, σ, is equal to the radial potential gradient at the pore wall (Gauss' law):

$$\xi = 1, \qquad \frac{\partial\psi}{\partial\xi} = \frac{z_+F}{\varepsilon RT}\bar{a}\sigma \tag{6}$$

b) At the pore center, the radial potential gradient is zero due to symmetry:

$$\xi = 0, \qquad \frac{\partial \psi}{\partial \xi} = 0 \tag{7}$$

So, ψ depends explicitly on ξ with $\bar{a}/\lambda$ and σ as parameters, and it can be evaluated for each given pair $(\bar{a}/\lambda,\sigma)$ by numerical resolution of Eq. (4) with Eqs. (6) and (7). The numerical method used here is explained in the Appendix.

In Fig. 1 we show the profile $\psi = \psi(r)$ for some values of $\bar{a}/\lambda$ (i.e., of $\bar{a}$ and $\bar{c}$) and σ. It is clear that the pore potential ψ at any given electrolytic concentration and charge density is less in the N01 membrane than in the N003 membrane.

The pore area-average electrical current,

$$I = \frac{2F}{} \int_0^{\bar{a}} (z_+ J_+(r,x) + z_- J_-(r,x)) r dr \tag{8}$$

and the pore area-average salt flux,

$$J = \frac{2}{\bar{a}^2} \int_0^{\bar{a}} (J_+(r,x) + J_-(r,x)) r dr \tag{9}$$

can be written, by means of Eqs. (1)–(7), as

$$I = L_{11}\left[- \frac{dE_m}{dx} \right] + L_{12} \frac{RT}{F} \left[- \frac{d \ln \bar{c}}{dx} \right] \tag{10}$$

and

$$J = L_{21}\left[- \frac{dE_m}{dx} \right] + L_{22} \frac{RT}{F} \left[- \frac{d \ln \bar{c}}{dx} \right] \tag{11}$$

where the coefficients L_{ij} are functions of definite integrals involving $\psi(\xi;\bar{a}/\lambda,\sigma)$:

$$L_{11} = \frac{2F^2}{RT} \int_0^1 \bar{c}(z_+^2 \nu_+ D_+ e^{-\psi} + z^2 \nu_- D_- e^{-z_- \psi / z_+}) \xi d\xi \tag{12}$$

$$L_{12} = L_{21} = \frac{2F}{RT} \int_0^1 \bar{c}(z_+ \nu_+ D_+ e^{-\psi} + z_- \nu_- D_- e^{-z_- \psi / z_+}) \xi d\xi \tag{13}$$

$$L_{22} = \frac{2}{RT}\int_0^1 \bar{c}(\nu_+ D_+ e^{-\psi} + \nu_- D_- e^{-z_-\psi/z_+})\xi d\xi \tag{14}$$

and therefore they can be calculated once the Poisson-Boltzmann equation has been solved.

Any electrokinetic parameter can be evaluated as some function of the L_{ij} coefficients. Our interest is focused here on the membrane potential which, from Eq. (10) with zero current condition, is

$$E_m(l) - E_m(0) = RT\int_{\ln \bar{c}_2} \frac{L_{21}}{L_{22}} d\ln \bar{c} \tag{15}$$

and on the saline permeability through the membrane, P_m, which, using Eqs. (10) and (11), can be expressed as

$$P_m \equiv \Pi\left[\frac{J_s}{\Delta \bar{c}}\right]_{I=0} = \Pi\left[\frac{J}{\Delta \bar{c}(\nu_+ + \nu_-)}\right]_{I=0} = \frac{\Pi RT}{l\Delta \bar{c}(\nu_+ + \nu_-)}\int_{\ln \bar{c}_2} \times \left(L_{22} - \frac{L_{12}^2}{L_{11}}\right) d\ln \bar{c} \tag{16}$$

where Π is the membrane porosity, J_s is the electroneutral salt flux, and Δ refers to a difference evaluated between the pore ends.

RESULTS AND DISCUSSION

We use here the membrane potentials and saline permeabilities previously measured in order to test the validity of the transport model that has been described before. These experimental results refer to two track-etched polycarbonate membranes whose pore diameters are 0.1 and 0.003 μm (N01 and N003 membranes) separating two electrolytic (LiCl or $MgCl_2$) aqueous solutions whose concentrations range from 0.1 to 100 mol/m^3. All the experiments have been carried out at 25.0°C.

In this study the steps followed have been:

a) The surface charge density on the pore walls, σ, has been evaluated from the experimental data on membrane potential for each membrane, solute, and pair of concentrations by fitting the right-hand side of Eq. (15) to them.
b) From these values of σ we predict the saline permeabilities, P_m^{theor}, and compare them with the corresponding experimental values, P_m^{exp}.

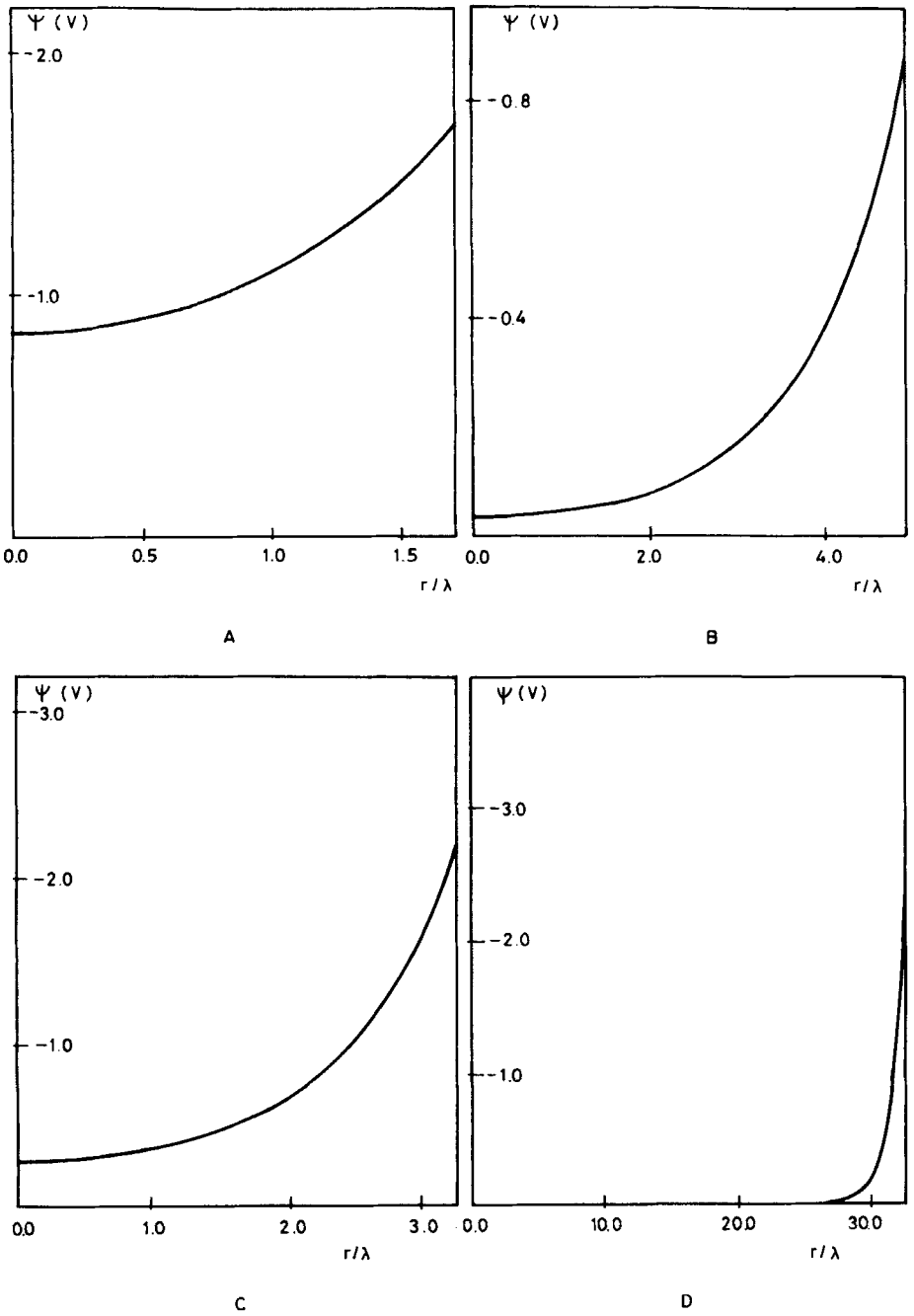

However, the directly measurable saline permeabilities are those of the membrane system (membrane plus both the adjacent diffusion layers), P_{ms}. So the P_m^{exp} values in Tables 1 and 2 have been obtained by assuming that the total diffusional resistance through the membrane system, R_t, is related both to the intrinsic membrane resistance, R_m, and to that of the boundary layers, R_δ, by

$$R_t = R_\delta(1) + R_m + R_\delta(2) \tag{17}$$

or, equivalently,

$$\frac{1}{P_{ms}} = \frac{\delta}{D_d(1)} + \frac{1}{P_m} + \frac{\delta}{D_d(2)} \tag{18}$$

where δ is the diffusion layers thickness (*4*) and $D_d(1)$ and $D_d(2)$ are the mean diffusion coefficients of the salt in the diffusion layers. The values of these diffusion coefficients for the mean concentrations in the layers have been taken from the literature (*6*).

In Tables 1 and 2 we see that P_m^{theor} agrees with P_m^{exp}. The small differences are chargeable to the important dispersion (*8*, *9*) of the membrane porosities affecting P_m^{exp} and to the approximate characterization of the effect of the diffusion layers in Eq. (18).

c) In Tables 1 and 2 we show the values of the relative permeability, P_m^{theor}/P_m^0 (i.e., nearly P_m^{exp}/P_m^0), where P_m^0 refers to the membrane permeability calculated for $\sigma = 0$.

From an analysis of these results, the influence of σ and $\bar{a}/\lambda$ (the two parameters of the model) on the relative permeabilities is concluded. This effect is slightly different for $MgCl_2$ and LiCl solutions.

It is seen that the relative permeability has a maximum for $\bar{a}/\lambda$ about 4, and decreases when $\bar{a}/\lambda$ moves away from this range. Actually, it would go to zero when $\bar{a}/\lambda$ did (great coion exclusion, and therefore little electroneutral transport) and to one when $\bar{a}/\lambda$ went to infinite (little relevance of the double layer in the pore, i.e., of the surface charge density on its wall).

FIG. 1. Radial profile of ψ in a cross section of the pore, determined by the given value of $\bar{c}$.

A) Membrane N003, Solute LiCl, $\bar{c}$ = 1.2 mol/m^3, σ = −0.0029 C/m^2
B) Membrane N003, Solute LiCl, $\bar{c}$ = 10 mol/m^3, σ = −0.0051 C/m^2
C) Membrane N003, Solute $MgCl_2$, $\bar{c}$ = 1.5 mol/m^3, σ = −0.0052 C/m^2
D) Membrane N01, Solute $MgCl_2$, $\bar{c}$ = 13 mol/m^3, σ = −0.023 C/m^2

TABLE 1

Values of P_m^{theor}, P_m^{exp}, and P_m^{theor}/P^0 for Some Pairs (c_1,c_2) of the Concentrations of the Bulk Solutions at Each Side of the Membrane ($c_1 \neq \bar{c}_1$ and $c_2 \neq \bar{c}_2$, $\bar{c}_1$ and $\bar{c}_2$ being the concentrations at the interfaces $x = 0$ and $x = l$ due to the diffusion layers). The Surface Charge Density, σ, Comes from the Experimental Results on the Membrane Potentials by Fitting Eq. (15). λ_{max} Refers to the Debye Length at $x = l$. The Solute Is LiCl

Membrane	c_1 (mol/m^3)	c_2 (mol/m^3)	$-\sigma$ (C/m^2)	$\bar{a}/\lambda_{max}$	$P_m^{theor} \times 10^6$ (m/s)	$P_m^{exp} \times 10^6$ (m/s)	P_m^{theor}/P_m^0
N01	1.00	0.505	0.0031	4.20	11.8	11.6	1.14
	2.01	1.00	0.0033	5.93	11.9	11.1	1.15
	4.01	2.02	0.0044	8.40	11.5	11.2	1.12
	8.02	4.00	0.0046	11.9	10.9	11.5	1.07
	16.0	8.06	0.0061	16.8	10.5	11.1	1.05
	31.9	16.0	0.0065	23.8	10.1	10.1	1.03
	63.5	32.0	0.0085	33.3	9.7	9.9	1.01
N003	1.01	0.500	0.0027	1.18	2.5	3.0	0.59
	2.01	1.01	0.0029	1.69	3.6	3.4	0.86
	3.98	2.00	0.0034	2.38	4.3	3.9	1.04
	6.87	3.38	0.0038	3.10	4.5	4.4	1.10
	13.7	6.83	0.0051	4.44	4.4	4.2	1.09
	27.2	13.7	0.0060	6.26	4.3	4.0	1.09
	57.2	28.9	0.0075	9.12	4.1	4.1	1.06

TABLE 2

Values of P_m^{theor}, P_m^{exp}, and P_m^{theor}/P^0 for Some Pairs (c_1,c_2) of the Concentrations of the Bulk Solutions at Each Side of the Membrane ($c_1 \neq \bar{c}_1$ and $c_2 \neq \bar{c}_2$, $\bar{c}_1$ and $\bar{c}_2$ being the concentrations at the interfaces $x = 0$ and $x = l$ due to the diffusion layers). The Surface Charge Density, σ, Comes from the Experimental Results on the Membrane Potentials by Fitting Eq. (15). λ_{max} Refers to the Debye Length at $x = 1$. The Solute Is $MgCl_2$

Membrane	c_1 (mol/m^3)	c_2 (mol/m^3)	$-\sigma$ (C/m^2)	$\bar{a}/\lambda_{max}$	$P_m^{theor} \times 10^6$ (m/s)	$P_m^{exp} \times 10^6$ (m/s)	P_m^{theor}/P_m^0
N01	0.535	0.266	0.0032	5.28	12.1	11.3	1.28
	1.08	0.54	0.0038	7.52	11.5	11.5	1.23
	2.15	1.08	0.0052	10.7	11.0	11.1	1.20
	4.31	2.15	0.0080	15.1	10.6	10.8	1.18
	8.70	4.30	0.0140	21.2	10.3	10.5	1.18
	17.3	8.60	0.023	30.1	9.8	10.2	1.16
	34.2	17.3	0.044	42.5	9.5	9.9	1.17
	69.0	34.2	0.067	60.2	8.8	9.8	1.14
N003	0.540	0.267	0.0026	1.47	2.2	2.3	1.02
	1.09	0.540	0.0023	2.09	2.5	2.3	1.17
	2.20	1.09	0.0027	2.97	2.5	2.2	1.19
	4.46	2.20	0.0034	4.23	2.4	2.2	1.17
	9.00	4.45	0.0052	6.03	2.3	2.1	1.15
	17.9	9.00	0.0082	8.57	2.2	2.1	1.14
	35.1	17.7	0.013	12.0	2.1	2.0	1.14
	67.0	34.1	0.021	16.7	2.0	2.0	1.14

d) In the framework of our model we have obtained the profiles of concentration, $\bar{c} = \bar{c}(x)$, and electrical potential, $E_m = E_m(x)$, inside the pores. Indeed, from Eqs. (10) and (11) and applying the zero current condition, we have

$$Jdx = \frac{RT}{\bar{c}}\left(L_{22} - \frac{L_{12}}{L_{11}}\right)d\bar{c} \tag{19}$$

which, integrated from $x = 0$, $\bar{c} = \bar{c}_1$ ($\bar{c}_1$ being the concentration at equilibrium with the bulk solution in $x = 0$), permits us to obtain $\bar{c} = \bar{c}(x)$.

Also, from Eq. (11) we have

$$E_m(x) = \int_{x=0}^{x} -\left(\frac{J}{L_{21}} + \frac{L_{22}}{L_{21}}\frac{RT}{\bar{c}(x)}\frac{d\bar{c}(x)}{dx}\right)dx \tag{20}$$

from which the profile of electric potential $E_m = E_m(x)$ can be obtained. Figure 2 show some relevant results on $\bar{c} = \bar{c}(x)$ and $E_m = E_m(x)$.

e) Finally, in Fig. 3 we see some profiles of the ionic concentrations, $c_+(r)$ and $c_-(r)$, obtained from Eq. (3). These profiles show the net charge of the solution in a pore cross section.

APPENDIX

Equation (4) is written as

$$\frac{\partial^2\psi}{\partial\xi^2} + \frac{1}{\xi}\frac{\partial\psi}{\partial\xi} = A[e^{a\psi} - e^{b\psi}] \tag{A-1}$$

By means of two series expansion of $e^{a\psi}$ and $e^{b\psi}$, this equation leads to

$$\frac{1}{A(a-b)}\frac{\partial^2\psi}{\partial\xi^2} + \frac{1}{A(a-b)}\frac{1}{\xi}\frac{\partial\psi}{\partial\xi} = \sum_{j=2}^{\infty}\frac{a^j - b^j}{j!}\frac{1}{a-b}\psi^j \tag{A-2}$$

that, with the change

$$y = \xi[A(a-b)]^{1/2}$$

become

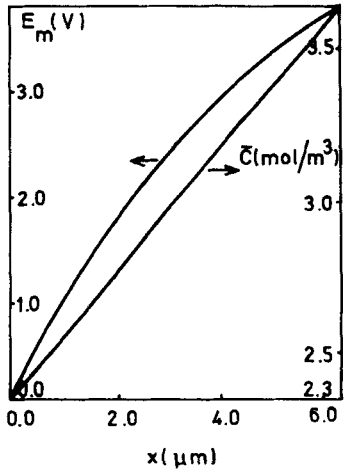

A

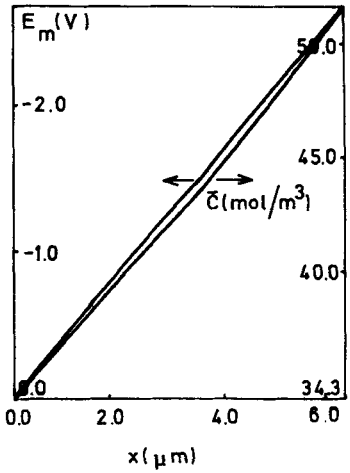

B

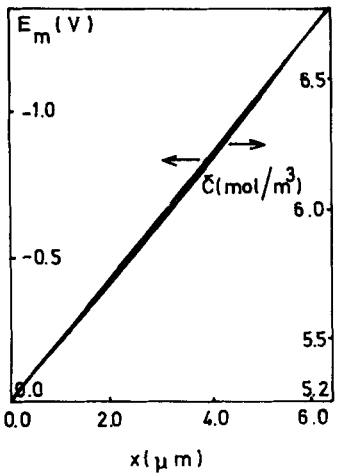

C

FIG. 2. Axial profiles of E_m and $\bar{c}$ inside the pore for some cases in Tables 1 and 2.

A) Membrane N003, Solute LiCl, $\sigma = -0.0034$ C/m^2
B) Membrane N003, Solute LiCl, $\sigma = -0.0075$ C/m^2
C) Membrane N01, Solute LiCl, $\sigma = -0.0046$ C/m^2

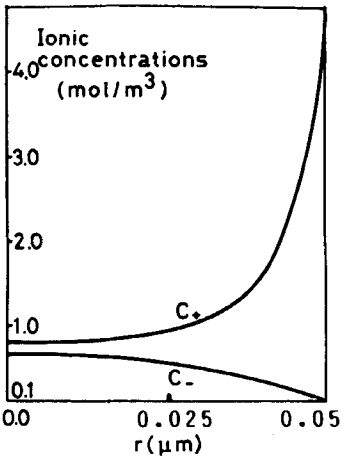

A

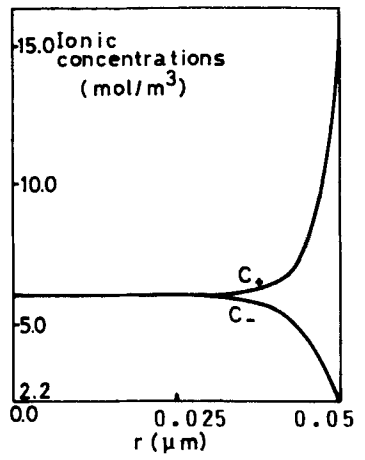

B

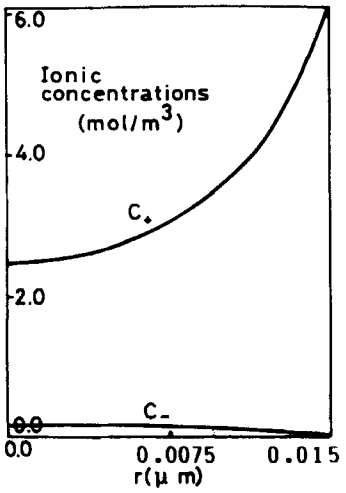

C

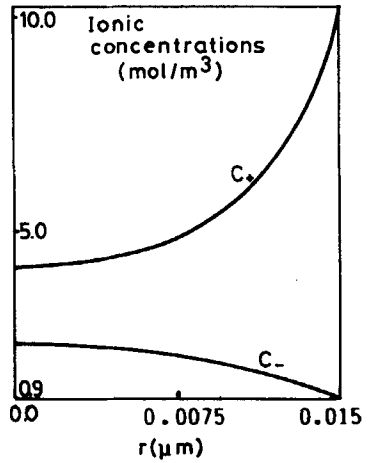

D

FIG. 1. See legend on page 256.

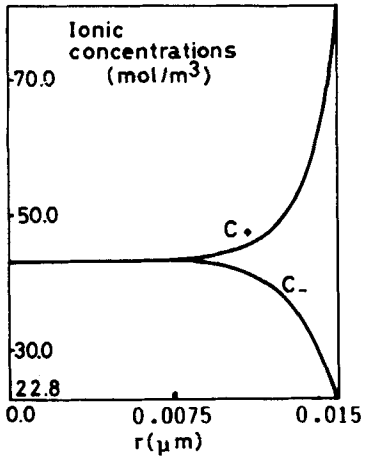

E

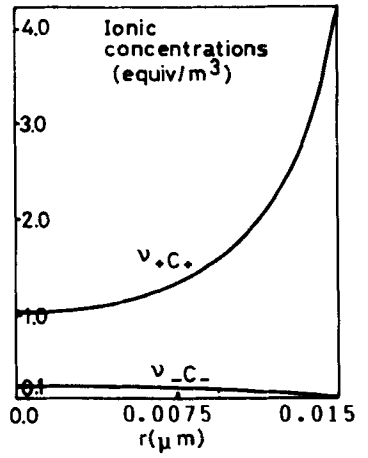

F

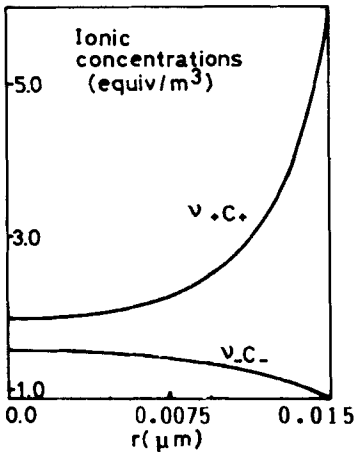

G

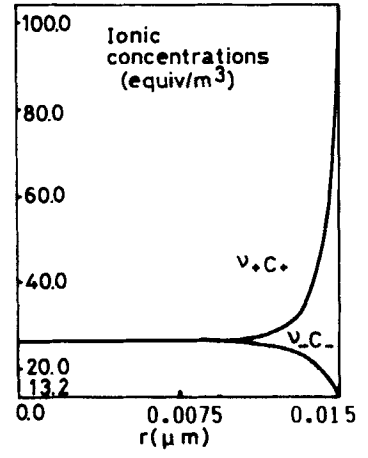

H

FIG. 1. See legend on page 256.

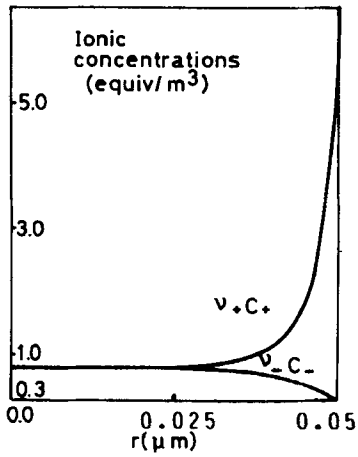

FIG. 3. Radial profiles of ionic concentrations in a cross section of the pore, determined by the value of $\bar{c}$, for some cases in Tables 1 and 2.

A) Membrane N01, Solute LiCl, $\bar{c}$ = 0.753 mol/m^3, σ = −0.0031 C/m^2
B) Membrane N01, Solute LiCl, $\bar{c}$ = 6.01 mol/m^3, σ = −0.0046 C/m^2
C) Membrane N003, Solute LiCl, $\bar{c}$ = 0.754 mol/m^3, σ = −0.0027 C/m^2
D) Membrane N003, Solute LiCl, $\bar{c}$ = 2.99 mol/m^3, σ = −0.0034 C/m^2
E) Membrane N003, Solute LiCl, $\bar{c}$ = 43.1 mol/m^3, σ = −0.0075 C/m^2
F) Membrane N003, Solute $MgCl_2$, $\bar{c}$ = 0.404 mol/m^3, σ = −0.0026 C/m^2
G) Membrane N003, Solute $MgCl_2$, $\bar{c}$ = 1.64 mol/m^3, σ = −0.0027 C/m^2
H) Membrane N003, Solute $MgCl_2$, $\bar{c}$ = 26.35 mol/m^3, σ = −0.013 C/m^2
I) Membrane N01, Solute $MgCl_2$, $\bar{c}$ = 0.81 mol/m^3, σ = −0.0038 C/m^2

$$\psi'' + \frac{1}{y}\psi' - \psi = \sum_{j=2}^{\infty} \frac{a^j - b^j}{j!} \frac{1}{a-b} \psi^j \qquad \text{(A-3)}$$

where ψ' and ψ'' are the first and second derivatives of ψ with respect to y, and ψ^j stands for the jth power of ψ. Since $(a^j - b^j)$ is divisible by $(a - b)$, the right-hand side of Eq. (A-3) is a polynomial in a and b.

On the other hand, ψ can be written as a double series:

$$\psi = \sum_{n,m=0}^{\infty} C_{nm} a^n b^m \psi_{nm} \qquad \text{(A-4)}$$

Then, substituting Eq. (A-4) in Eq. (A-3) and equating the terms of the same order in $a^n b^m$, we get

$$\psi''_{00} + \frac{1}{y}\psi'_{00} - \psi_{00} = 0$$

$$\psi''_{10} + \frac{1}{y}\psi'_{10} - \psi_{10} = G_{10}(\psi_{00})$$

$$\psi''_{01} + \frac{1}{y}\psi'_{01} - \psi_{01} = G_{01}(\psi_{00}) \qquad \text{(A-5)}$$

$$\cdots\cdots\cdots\cdots\cdots$$

$$\psi''_{nm} + \frac{1}{y}\psi'_{nm} - \psi_{nm} = G_{nm}(\psi_{00}, \psi_{10}, \ldots, \psi_{n-1,m-1})$$

The boundary conditions given by Eqs. (6) and (7) in terms of y are

$$\psi'(0) = 0 \qquad \text{(A-6)}$$

$$\psi'(y_{\max}) = S \qquad \text{with } S = \frac{Fz_+\bar{a}}{\varepsilon RT[A(a-b)]^{1/2}} \qquad \text{and } y_{\max} = [A(a-b)]^{1/2} \qquad \text{(A-7)}$$

The linear differential equations in the System (A-5) can be solved by a parameters-variation method (*10*). We look for solutions accomplishing:

$$\psi'_{nm}(0) = 0, \qquad \text{for all } n,m$$
$$\psi_{nm}(0) = 0, \qquad \text{for all } n,m > 0 \qquad \text{(A-8)}$$

with

$$\psi_{nm}(y) = I_0(y)\int_0^y \frac{-K_0(y_1)G_{nm}(y_1)}{W(I_0(y_1),K_0(y_1))}\,dy_1 + K_0(y)\int_0^y \frac{I_0(y_1)G_{nm}(y_1)}{W(I_0(y_1),K_0(y_1))}\,dy_1 \qquad \text{(A-9)}$$

where I_0 and K_0 are the Bessel functions which are solutions of the homogeneous part of each equation in (A-5) (*11*), and

$$W(I_0(y_1),K_0(y_1)) = -1/y_1 \qquad \text{(A-10)}$$

is the Wronskian of $I_0(y_1)$ and $K_0(y_1)$.

So the zero-order approximation for the solution (Eq. A-4) is

$$\psi(y) \simeq \psi_0(y) = \frac{S}{I_1(y_{max})} I_0(y) \tag{A-11}$$

where Eq. (A-7) has been taken into account and I_1 is the Bessel function of order 1. In the same way, the first-order approximation is

$$\psi(y) \simeq \psi_1(y) = u_1\psi_0(y) + \tfrac{1}{2}(a + b)u_1^2\psi_{10}(y) \tag{A-12}$$

where

$$\psi_{10}(y) = I_0(y)\int_0^y y_1 K_0(y_1)\psi_0^2(y_1)dy_1 - K_0(y)\int_0^y y_1 I_0(y_1)\psi_0^2(y_1)dy_1 \tag{A-13}$$

and u_1 is the solution of the polynomial,

$$\tfrac{1}{2}(a + b)u_1^2\psi'_{10}(y_{max}) + u_1\psi'_0(y_{max}) - S = 0 \tag{A-14}$$

Higher order approximations may be obtained in the same way. The convergence of the method is tested by comparing each approximation with the following one. The differences between ψ_5 and ψ_6 are negligible in all cases studied, and this is why we have always taken $\psi = \psi_6$.

REFERENCES

1. R. P. Buck, "Kinetics of Bulk and Interfacial Ionic Motion: Microscopic Bases and Limits for the Nernst-Planck Equation Applied to Membrane Systems," *J. Membr. Sci., 17,* 145 (1984).
2. T. R. Brumleve and R. P. Buck, "Potential Reversals across Site-Free Passive Membranes. A Simulation Analysis," *J. Electroanal. Chem., 126,* 55 (1981).
3. H. Cohen and J. W. Cooley, "The Numerical Solution of the Time-Dependent Nernst-Planck Equations," *Biophys. J., 5,* 145 (1965).
4. L. Martínez, A. Hernández, and F. Tejerina, "Concentration Dependence of Some Electrochemical Properties of Polycarbonate Microporous Membranes and Evaluation of Its Electrokinetic Charge," *Sep. Sci. Technol., 22,* 1625 (1987).
5. G. B. Westerman-Clark and J. L. Anderson, "Experimental Verification of the Space Charge Model for Electrokinetics in Charged Microporous Membranes," *J. Electrochem. Soc., 130,* 839 (1983).
6. W. H. Koh and H. P. Silverman, "Anion Transport in Thin-Channel Cation Exchange Membranes," *J. Membr. Sci., 13,* 279 (1983).
7. R. A. Robinson and R. M. Stokes, *Electrolyte Solutions,* 2nd ed., Butterworths, London, 1959.
8. W. John, S. Hering, and G. Sasaki, "Characteristics of Nuclepore Filters with Large Pore Size. I. Physical Properties," *Atmos. Environ., 17,* 115 (1983).

9. F. Martinez-Villa, J. I. Arribas, and F. Tejerina, "Quantitative Microscopical Study of Surface Characteristic Parameters in Track-Etched Membranes," *J. Membr. Sci.,* In Press.
10. F. Simmons, *Differential Equations with Applications and Historical Notes,* McGraw-Hill, New York, 1972.
11. M. Abramowitz and I. A. Stegun, *Handbook of Mathematical Functions,* Dover Publications, New York, 1970.

Received by editor February 23, 1987